

FC

B R L

BRL CR 295

(12)

AD

ADA 023687

CONTRACT REPORT NO. 295

FRACTURE MODELING IN THE SMITE CODE

Prepared by

Mathematical Applications Group, Inc.
3 Westchester Plaza
Elmsford, NY 10523



March 1976

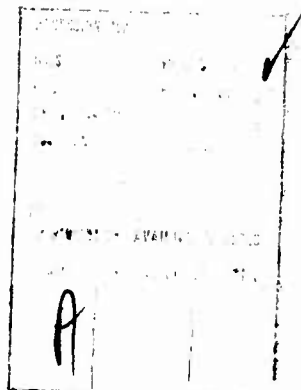
Approved for public release; distribution unlimited.

USA BALLISTIC RESEARCH LABORATORIES
ABERDEEN PROVING GROUND, MARYLAND

Destroy this report when it is no longer needed.
Do not return it to the originator.

Secondary distribution of this report by originating
or sponsoring activity is prohibited.

Additional copies of this report may be obtained
from the National Technical Information Service,
U.S. Department of Commerce, Springfield, Virginia
22151.



The findings in this report are not to be construed as
an official Department of the Army position, unless
so designated by other authorized documents.

UNCLASSIFIED

SECURITY CLASSIFICATION OF THIS PAGE (When Data Entered)

REPORT DOCUMENTATION PAGE		READ INSTRUCTIONS BEFORE COMPLETING FORM
1. REPORT NUMBER <i>(18) BRL CONTRACTOR REPORT NO. - 295</i>	2. GOVT ACCESSION NO.	3. RECIPIENT'S CATALOG NUMBER
4. TITLE (and Subtitle) Fracture Modeling in the SMITE Code.	5. TYPE OF REPORT & PERIOD COVERED <i>(9) Final rept.</i>	
6. AUTHOR(s) S. Z. Burstein H. S. Schechter	7. PERFORMING ORG. REPORT NUMBER P-7111	
8. CONTRACT OR GRANT NUMBER(s) <i>(10) DAAD05-75-C-0741 NEW</i>	9. PERFORMING ORGANIZATION NAME AND ADDRESS Mathematical Applications Group, Inc. 3 Westchester Plaza Elmsford, NY 10523	
10. PROGRAM ELEMENT, PROJECT, TASK AREA & WORK UNIT NUMBERS	11. CONTROLLING OFFICE NAME AND ADDRESS US Army Ballistic Research Laboratories Aberdeen Proving Ground, MD 21005 <i>(11) 2PP</i>	
12. REPORT DATE <i>(12) MARCH 1976</i>	13. NUMBER OF PAGES 28	
14. MONITORING AGENCY NAME & ADDRESS (if different from Controlling Office) US Army Materiel Development and Readiness Command 5001 Eisenhower Avenue Alexandria, VA 22333	15. SECURITY CLASS. (of this report) <i>(13) UNCLASSIFIED</i>	
16. DISTRIBUTION STATEMENT (of this Report) <i>Approved for public release; distribution unlimited.</i>	15a. DECLASSIFICATION/DOWNGRADING SCHEDULE	
17. DISTRIBUTION STATEMENT (of the abstract entered in Block 20, if different from Report)		
18. SUPPLEMENTARY NOTES		
19. KEY WORDS (Continue on reverse side if necessary and identify by block number) nucleation crack growth brittle fracture ductile failure numerical modeling		
20. ABSTRACT (Continue on reverse side if necessary and identify by block number) This report documents the incorporation of the Stanford Research Institute's NAG-FRAG model into the SMITE code, a second order, Eulerian finite difference scheme modeling elasto-plastic material response to impact. Sample computations are presented.		

TABLE OF CONTENTS

I.	INTRODUCTION	5
II.	FRACTURE MODIFICATIONS TO SMITE . . .	6
III.	INPUT	8
IV.	DUCTILE FRACTURE RESULTS.	13
V.	SUMMARY AND RECOMMENDATIONS	20
	DISTRIBUTION LIST	21

I. INTRODUCTION

The reader is assumed to be familiar with the axisymmetric version of the SMITE code which is described fully in BRL CR-255. It is also assumed that the reader is familiar with the Stanford Research Institute (SRI) ductile fracture subroutine, DFRACT, and brittle fracture subroutine, BFRACT. The description of the theory of fracture used in these routines are contained in AMMRC CTR 75-2 and BRL CR-222.

The purpose of this research effort was twofold:

- (i) First to modify the SMITE code so that the ductile and brittle fracture model (that of SRI) could be incorporated into SMITE.
- (ii) Compare results obtained with the modified code with the Lagrangian formulation of SRI.

The modifications introduced into the SMITE code to incorporate the fracture subroutines are described in the following section. Each subroutine that required changes is described.

II. FRACTURE MODIFICATIONS TO SMITE

DENSB - Since pressure is now carried as an explicit variable, the pressure on the free surface is set to that necessary to produce zero normal stress. The iteration of density to obtain the required pressure through the solid equation of state is removed.

FDIFF - Logic is added to call IFRACT and hence obtain the relative properties from the fracture subroutines once the critical pressure has been exceeded at a point.

IFRACT - This is the routine that actually incorporates the fracture subroutine DFRACT or BFRACT. This is accomplished by introducing a quasi-Lagrangian calculation into the Eulerian code. Once the velocities at the advanced time are obtained at a mesh point by the two step method, they are integrated backwards in time to determine where that mesh point came from in a Lagrangian sense. Values of all variables at the initial time are then assigned to this point by linear interpolation from surrounding points. The ductile fracture subroutine DFRACT or the brittle fracture subroutine BFRACT may then be called to update these values to the original mesh point at the advanced time.

Values for strain are obtained by numerically differentiating the velocities using central differences. An α acceleration at a point with index i , for instance, may be obtained by differencing velocities at points $i-1$ and $i+1$. If the Lagrangian point lies between mesh lines i and $i+1$, acceleration at $i+1/2$ may also be obtained by differencing velocities at points i and $i+1$. Similar differencing is used to obtain β accelerations. Accelerations at the Lagrangian point are then evaluated by interpolation. The necessary strains are obtained by transforming from α , β to z , r space.

INFACE - The pressure on both sides of the interface is set to that necessary to produce a continuous normal stress. The iteration of density to obtain the required pressure through the solid equation of state is removed.

INITAL - The number of dependent variables is changed to 10 for ductile fracture and 22 for brittle fracture. Seven parameters are read in for ductile fracture and fourteen for brittle fracture.

INTRPL - Coding is added to reflect the additional variables about the axis of symmetry.

OUTPUT - Coding is added to print the additional variables at points where fracture has occurred.

PLTOUT - The output of points that are in the plastic region is removed and the amount of damage to fractured points is substituted.

PRS - The solid equation of state is changed to the Mie-Gruneisen equation.

$$P = (C\mu + D\mu^2 + S\mu^3)(1 - \frac{\Gamma\mu}{2}) + r\rho E$$

where C, D, S are constants, Γ is the Gruneisen ratio, E is the internal energy, ρ is the density and $\mu = \rho/\rho_0 - 1$. In the next section, we describe the modifications required for input data preparation.

III. INPUT

There are three types of input data, integer (I), real (R) and alphanumeric (A). An integer is a number without a decimal point which must be right justified in its field. A real number has a decimal point which may be followed by an exponent of the form E±N. The ±N represents the power of 10 by which the number is to be multiplied. The + may be omitted if N is positive and the E need not appear if either the + or - is present. If an exponent is present it must be right justified in the field. Alphanumeric input consists of exactly the punched characters and blanks appearing in the field. A description of the necessary input data for SMITE follows. The card number refers to the type of input. If more than one card is necessary for this input, there may be several cards of the same type number.

CARD	COLS.	TYPE	NAME	DESCRIPTION
1	1-80	A	TITLE	Any alphanumeric information to be printed at the beginning of the output.
2	1-10 11-20 21-30 31-40 41-50	R	TMAX TPRIN TPRPL TPLOT TSAVE	Maximum problem time in microseconds. Print output increment in microseconds. Printer plot output increment in microseconds. Plot tape output increment in microseconds. Restart tape output increment in microseconds. If any output increment is negative that output is suppressed.
	51-60	R	TCOMP	Maximum computation time in seconds.
	61-70	R	PORG	Value in centimeters of axial coordinate at left center of printer plot. The radial coordinate is set to zero.
	71-80	R	PSCL	Scale of printer plot in centimeters per inch.
3	1-10	R	RDIS	Minimum fractional mesh allowed. If a point is closer to the boundary than this fraction of mesh size, interpolation will be used.
4	1-5 6-10	I	NMAT ISTART	Number of materials. Restart flag. Zero for initial run, otherwise non zero.
5	1-5	I	NINFC	Number of material interfaces. Use 0 if there is only one material and omit card 6.
6	1-5 6-10 11-15 16-20 21-25 26-30 31-35 36-40 41-45 46-50 51-55 56-60	I	INF(1) INF(2) INF(3) INF(4) INF(5) INF(6) INF(7) INF(8) INF(9) INF(10) INF(11) INF(12)	Index of dominant material of interface. Boundary of this material defines interface. Index of first boundary point on interface. Index of last boundary point on interface. Index of second material of interface. Interface boundary of this material replaced by interface boundary of first material. Index of last boundary point on interface. Index of first boundary point on interface. Index of dominant material of next interface, etc. This sequence is repeated, six entries per interface, two interfaces per card until all interfaces have been defined. The boundary point indices refer to the points defining the material boundaries in the order in which they are input.

The set of cards containing the input parameters for the individual materials follows. This entire set is repeated for each material until all materials have been defined.

CARD	COLS.	TYPE	NAME	DESCRIPTION
7	1-5 6-10 11-15 16-20 21-25	I I I I I	NI NJ IP IL JF	Maximum number of mesh lines allowed in axial direction. Maximum number of mesh lines allowed in radial direction. First axial index interior to domain. Last axial index interior to domain. First radial index interior to domain. Must be 1 if domain touches axis and greater than 1 otherwise.
	26-30	I	JL	Last radial index interior to domain. At least one mesh line must be exterior to the material on all sides (except at axis). Additional exterior mesh lines should be allowed in the directions that the material will move. If the material reaches the end of the allowed mesh in one direction and there is exterior mesh in the opposite direction, it will be automatically shifted.
	31-35 36-40 41-45 46-50 51-55 56-60	I I I I I I	NLP NTP NRT NPMAX NTR MATNO	Number of points in first boundary segment. Number of points in second boundary segment. Number of points in third boundary segment. Maximum number of boundary points allowed. Number of tracer particles. Material property number. If positive equation of state constants set in program, if negative they are input.
10	61-65 66-70	I I	IPRINT JPRINT	Maximum number of interior points printed in axial direction. If positive count from leftmost interior point, if negative count from rightmost interior point. Maximum number of interior points printed in radial direction. If positive count from lowest interior point, if negative count from highest interior point. If either IPRINT or JPRINT is zero no interior points will be printed.
8	1-10 11-20 21-30 31-40 41-50	R R R R R	ZLEN YMAX THETA CAP D	Initial axial length in centimeters. Initial radial length in centimeters. 89.5 1.0E4 Radial length of densest mesh spacing. Radial mesh will be fairly uniform for this length and will then increase in size. Not used.
	51-60 61-70 71-80	R R R	VIS VIST CFL	Viscosity coefficient for wostep equations. Should be between zero and two. Fraction of computed time step used. A safety factor usually between 0.5 and 0.8.

CARD	COLS.	TYPE	NAME	DESCRIPTION
9	1-10	R	MU	Shear modulus in 10^{12} dynes/cm ² .
	11-20	R	YC	Yield strength in tension in 10^{12} dynes/cm ² .
	21-30	R	RHO	Initial density in grams/cm ³ .
	31-40	R	UI	Initial axial velocity in centimeters/microsecond.
	41-50	R	VI	Initial radial velocity in centimeters/microsecond.
10	1-10	R	APL	Gruneisen ratio in equation of state.
	11-20	R	BFL	C - dynes/cm ²
	21-30	R	APB	D - dynes/cm ²
	31-40	R	BFB	E - dynes/cm ²
	41-50	R		Not used
	51-60	R		Not used
	61-70	R		Not used
	71-80	R		Not used
10a	1-10	R		Not used
	11-20	R	FMIN	Maximum tensile stress permitted, dynes/cm ² .
11	1-10	R	TSR(1)	Growth constant - cm ² /dyn/sec.
	11-20	R	TSR(2)	Growth threshold - dyn/cm ² .
	21-30	R	TSR(3)	Nucleation radius parameter - cm.
	31-40	R	TSR(4)	Parameter in nucleation function - no./cm ³ /sec.
	41-50	R	TSR(5)	Nucleation threshold - dyn/cm ² .
	51-60	R	TSR(6)	Parameter in nucleation function - dyn/cm ² .
	61-70	R	TSR(7)	Not used.
	71-80	R	TSR(8)	Threshold stress for entering BRACT.
11a	1-10	R	TSR(9)	0 for stress, 1 for deviator stress
	11-20	R	TSR(10)	Ratio c, number of fragments to number of cracks.
	21-30	R	TSR(11)	Ratio of fragment radius to crack radius.
	31-40	R	TSR(12)	Value of crack volume which defines threshold of coalescence.
	41-50	R	TSR(13)	TF, where fragment volume = TF (RF) ³
	51-60	R	TSR(14)	Not used.

TSR(8) - TSR(14) may be left blank for ductile fracture.

CARD	COLS.	TYPE	NAME	DESCRIPTION
12	1-10	R	FRX(I)	Axial coordinate in centimeters of first point of boundary.
	11-20	R	FRY(I)	Radial coordinate in centimeters of first point of boundary.
	21-30	R	FRX(I)	Axial coordinate of second point.
	31-40	R	FRY(I)	Radial coordinate of second point.
	41-50	R	FRX(I)	This sequence is repeated, four points per card, until the entire boundary has been input.
	51-60	R	FRY(I)	
61-70	R		FRX(I)	If the boundary touches the axis of symmetry, the defining points must start and end on the axis of symmetry. If the boundary does not touch the axis, the first and last points should be the same and should be on a part of the boundary that will never become a material interface.
71-80	R		FRY(I)	
13	1-5	I	ITR	Index of first boundary point selected as tracer.
	6-10	I	ITR	Index of second boundary point selected.
	11-15	I		
	16-20	I		This sequence is repeated, sixteen indices per card until all tracer particles are selected. The boundary point indices refer to the points defining the material boundary in the order in which they are input. These tracer points will be tagged with their input number on this card and their position in time will be traced throughout the run.
	21-25	I		
	25-30	I		
	31-35	I		
	36-40	I		
	41-45	I		
	46-50	I		
	51-55	I		
	56-60	I		
	61-65	I		
	66-70	I		
	71-75	I		
	76-80	I		

IV. DUCTILE FRACTURE RESULTS

A tapered flyer plate, Aluminum-1145, impacting on a flat plate, Aluminum-1145, at a striking velocity $v_g = .0163 \text{ cm}/\mu\text{-sec}$. was chosen as a test case. It is, except for the cylindrical geometry, similar to the problem run by SRI which, in that case, was specified in plane coordinates. The coordinate mesh chosen for the computation presented here is not the finest possible but is similar to the SRI mesh.

The target had a mesh spacing $\Delta z = L/20$ where the thickness $L = 0.316 \text{ cm}$. The spacing of the mesh in the radial direction $\Delta r = h/40$ where the height of the target is $h = 1.184 \text{ cm}$. In the tapered flyer plate the mesh spacing in z , $\Delta z = 0.158 \text{ cm}/12$; the radial mesh increment is $\Delta r = 0.592 \text{ cm}/24$.

The following table gives the parameters (data card 10b) used in the nucleation and fracture model:

FRACTURE PARAMETERS: Aluminum-1145

Growth Constant	-0.01
Growth Threshold	$-0.4 \cdot 10^{10}$
Nucleation Radius	$0.1 \cdot 10^3$
N_0	$0.3 \cdot 10^{10}$
Nucleation Threshold	$-0.3 \cdot 10^{10}$
P_1	$-0.4 \cdot 10^9$

The results of the computation for the value of the parameters given in the above table is presented in the three accompanying figures. Figure 1 shows the geometrical configuration at the moment of impact, $t=0$. At $t=1.464 \mu\text{sec}$., shown in Figure 2, the target shows the presence of an internal fracture centered about the center line of the plate. This fractured region represents a percent fracture volume between 5 to 12 percent.

The presence of this fracture island is similar to that obtained by SRI, however their calculation was carried out with the brittle model for a flyer plate/target configuration with the material properties of Armco iron. As a result, due to the higher growth rates of this brittle material, the fracture island was of much greater extent, a reasonable result (see the Table below). The last figure shows, at $t=2.198\mu\text{-sec.}$, that there is virtually no continued growth of the fracture island.

FRACTURE PARAMETERS: Armco Iron

Growth Constant	$-0.12 \cdot 10^{-3}$
Growth Threshold	0.
Nucleation Radius	$0.4 \cdot 10^{-2}$
\dot{N}_0	$0.5 \cdot 10^9$
Nucleation Threshold	$1.12 \cdot 10^{11}$
P_1	$-7.4 \cdot 10^9$

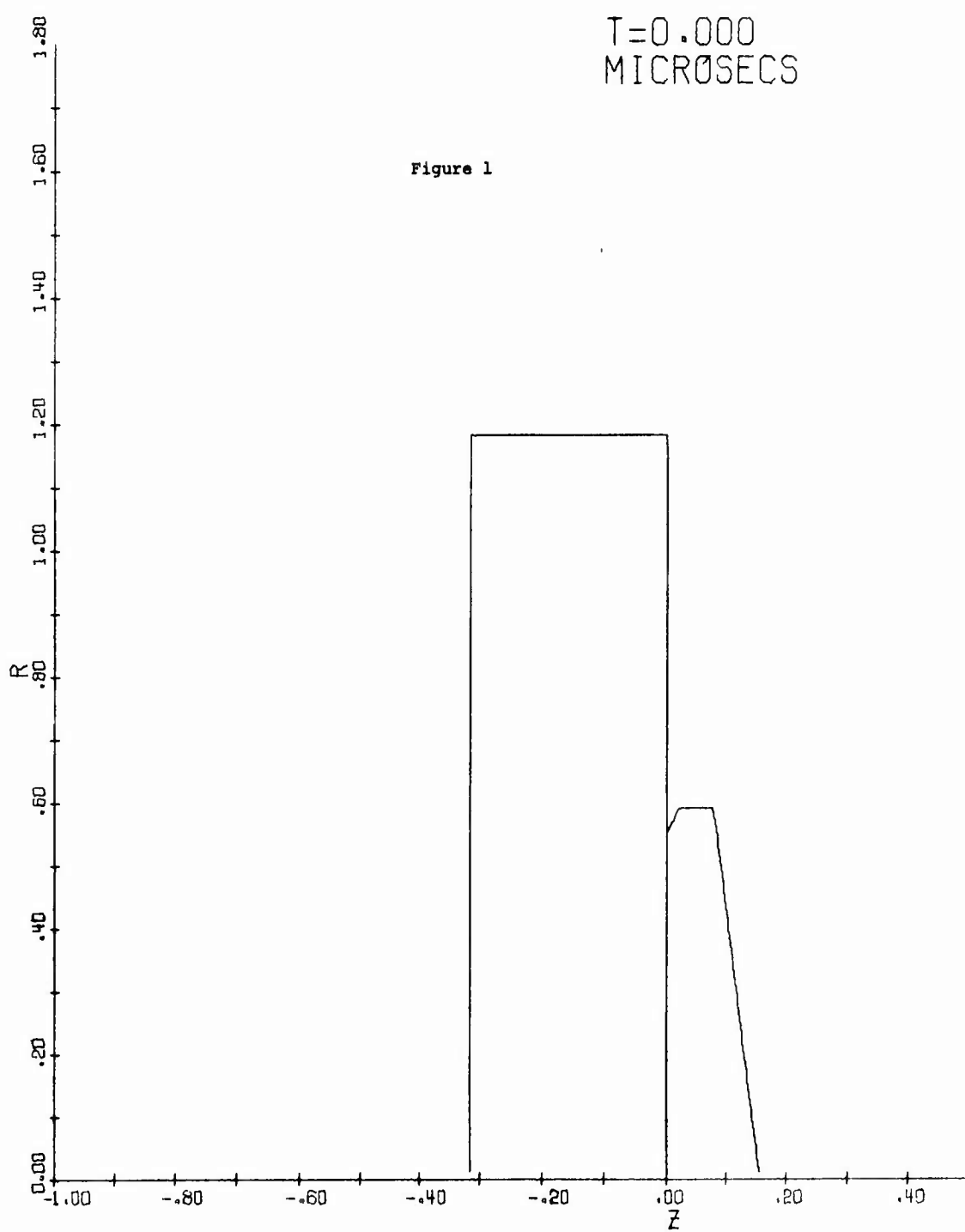
The brittle fracture routine was substituted for the ductile fracture routine, and the axisymmetric flyer plate problem was run with Armco iron properties rather than Aluminum-1145 properties. At this point, we have very limited results. The main difficulty is a convergence problem in the brittle fracture subroutine. We have been conversing with the scientific staff at SRI who are responsible for the brittle fracture model. As a result of their suggestions, there has been improvement in the convergence of the iterative procedure in BFRACI but not a complete solution to the problem.

DUCTILE FRACTURE-AL 1145
 6.0 1.46 0.73 0.73 -0.73 1500.0 -1.0 0.25
 0.5
 2 0
 1
 2 1 2 1 5 4
 23 41 2 21 1 40 2 2 3 300 1 -1 999 999
 0.3156 1.184 89.5 1000.0 1.184 0.0 0.0 0.0 0.0 0.65
 0.3 0.002 2.7 0.0 0.0 0.0 0.0 0.0 0.0 0.0
 2.04 0.76 1.5 0.0 0.0 0.0 0.0 0.0 0.0 0.0
 0.0 -9.999 -1.0 E=2 -4.0 E9 1.0 E=4 3.0 E9 -3.0 E9 -4.0 E8 0.0
 -0.3156 0.0 -0.3156 1.184 0.0 1.184 0.0 0.0 0.0 0.55
 0.0 0.0
 1
 16 29 4 15 1 24 2 3 2 250 1 -2 999 999
 0.1578 0.592 89.5 1000.0 0.592 0.0 0.0 0.0 0.0 0.65
 0.3 0.002 2.7 -0.0163 0.0 0.0 0.0 0.0 0.0 0.0
 2.04 0.76 1.5 0.0 0.0 0.0 0.0 0.0 0.0 0.0
 0.0 -9.999 -1.0 E=2 -4.0 E9 1.0 E=4 3.0 E9 -3.0 E9 -4.0 E8 0.0
 0.0 0.0 0.0 0.55 0.02 0.592 0.0789 0.0 0.592
 0.1578 0.0
 1

BRITTLE FRACTURE-STEEL=2151-3
 6.0 1.0 1.0 1.0 -2.0 500.0 +1.0 0.2
 0.5
 2 0
 1
 2 1 2 1 5 4
 16 31 2 15 1 30 2 2 3 300 1 -1 999 999
 0.4233 1.0 89.5 1000.0 1.0 0.0 0.0 0.0 0.0 0.0 0.0 0.65
 0.819 0.01035 7.85 0.0 0.0 0.0 0.0 0.0 0.0 0.0 0.0 0.0
 1.69 1.589 5.17 51.7 0.0 0.0 0.0 0.0 0.0 0.0 0.0 0.0
 0.0 -9.999 4.0 E=3 5.0 E8 +1.12 E10 -7.4 E8 0.0 0.0
 -1.2 E=4 0.0 0.25 1.0 0.2 1.0 0.0 0.0 0.0 0.0 0.0 0.0
 -0.4233 0.0 -0.4233 1.0 0.0 0.0 1.8 0.0 0.0 0.0 0.0 0.85
 0.0 0.0
 1
 23 32 3 22 1 30 2 3 2 200 1 -1 999 999
 0.3048 0.9 89.5 1000.0 0.9 0.0 0.0 0.0 0.0 0.0 0.0 0.65
 0.819 0.01035 7.85 -0.05 0.0 0.0 0.0 0.0 0.0 0.0 0.0 0.0
 1.69 1.589 5.17 51.7 0.0 0.0 0.0 0.0 0.0 0.0 0.0 0.0
 0.0 -9.999 4.0 E=3 5.0 E8 +1.12 E10 -7.4 E8 0.0 0.0
 -1.2 E=4 0.0 0.25 1.0 0.2 1.0 0.0 0.0 0.0 0.0 0.0 0.9
 0.0 0.0 0.0 0.0 0.85 0.01 0.9 0.0762 0.9
 0.3048 0.0
 1

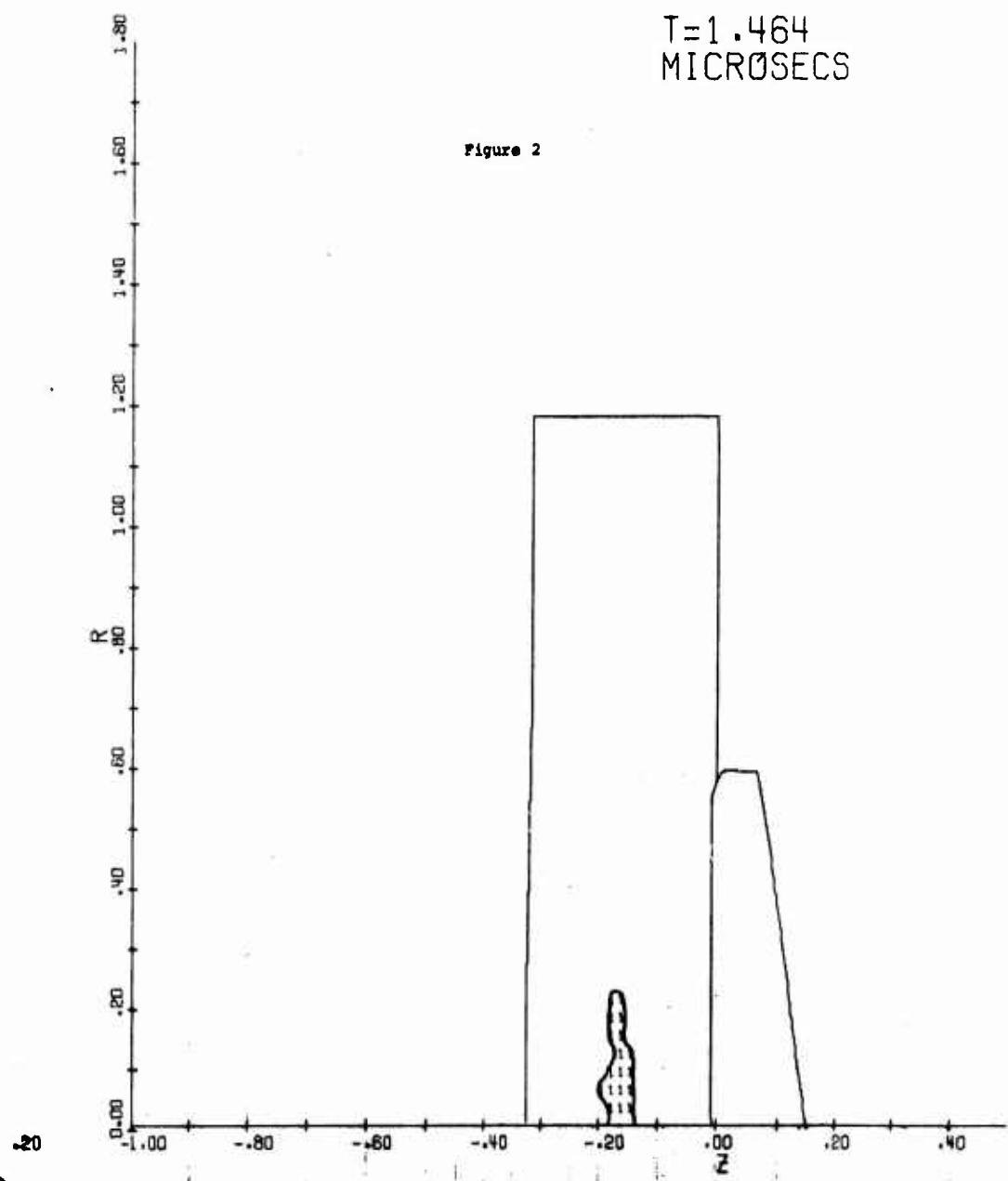
$T = 0.000$
MICROSECS

Figure 1



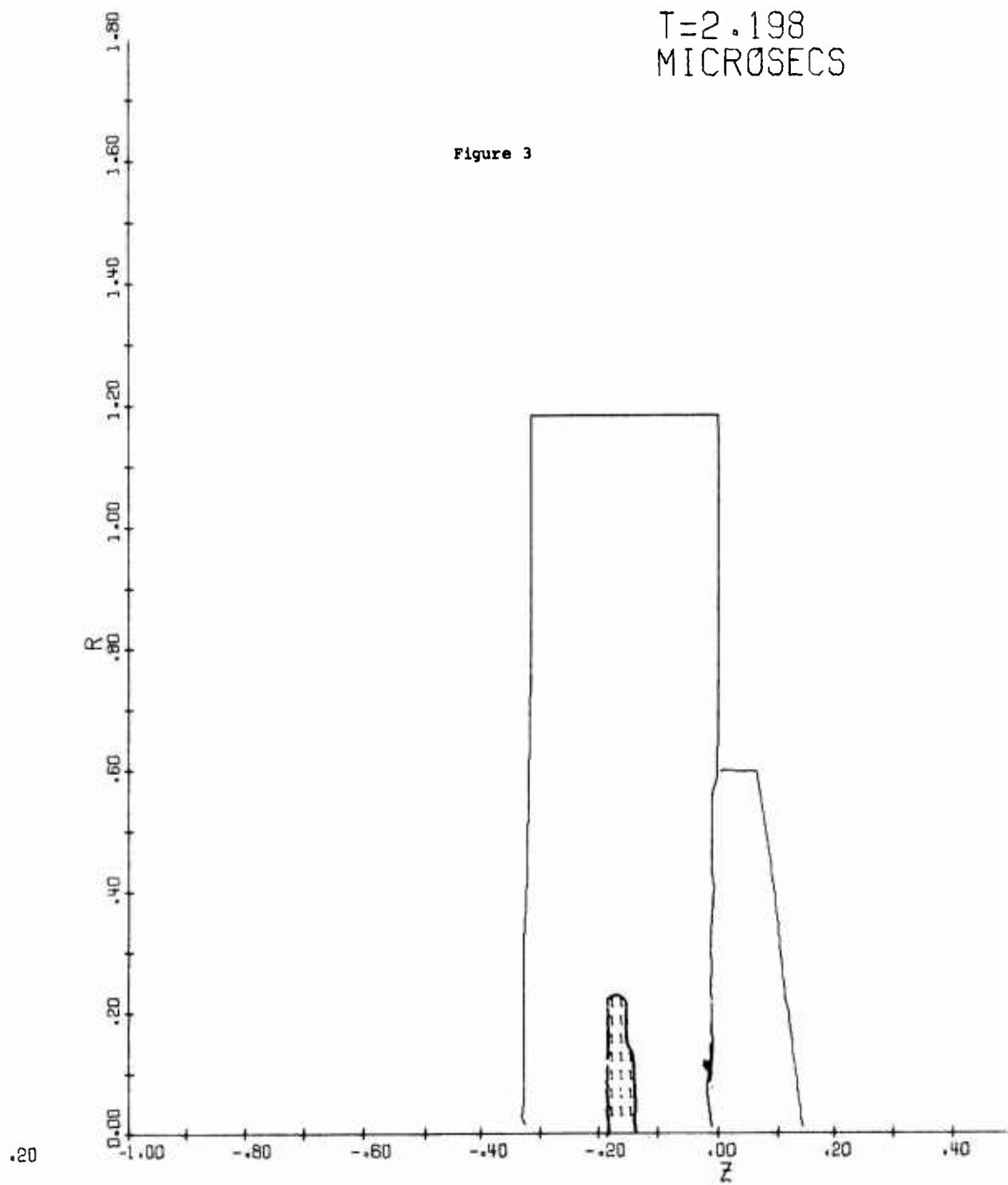
$T = 1.464$
MICROSECS

Figure 2



$T = 2.198$
MICROSECS

Figure 3



V. SUMMARY AND RECOMMENDATIONS

The feasibility of adapting the SRI Lagrangian fracture subroutines for inclusion in the SMITE Eulerian code has been demonstrated. The ductile fracture subroutine was successfully run with reasonable results. The brittle fracture subroutine was run, but aborted due to convergence problems. SRI was consulted about the problem and recommended corrections were received. However, the corrections were not received until after the funds under the present contract were expended. Those corrections, therefore, have not been included in the code.

It is recommended that the following additional items be considered by BRL:

- 1) Inclusion and testing of the corrections recommended by SRI with additional consultation, if necessary.
- 2) More extensive testing of both the ductile and brittle fracture subroutines to determine if any further corrections are necessary.
- 3) Further modification of printed and graphic output to present results in a form suitable to the requirements of BRL.

DISTRIBUTION LIST

<u>No. of Copies</u>	<u>Organization</u>	<u>No. of Copies</u>	<u>Organization</u>
12	Commander Defense Documentation Center ATTN: DDC-TCA Cameron Station Alexandria, VA 22314	2	Commander US Army Electronics Command ATTN: DRSEL-HL-CT Mr. S. Crossman DRSEL-RD Fort Monmouth, NJ 07703
1	Director Defense Nuclear Agency ATTN: MAJ T. Stong Arlington, VA 22209	2	Commander US Army Missile Command ATTN: DRSMI-R DRSMI-RBL Redstone Arsenal, AL 35809
1	Director Defense Advanced Research Projects Agency ATTN: Tech Info 1400 Wilson Boulevard Arlington, VA 22209	1	Commander US Army Tank Automotive Logistics Command ATTN: DRSTA-RHFL Warren, MI 48090
1	Commander US Army Materiel Development and Readiness Command ATTN: DRCDMA-ST 5001 Eisenhower Avenue Alexandria, VA 22333	4	Commander US Army Mobility Equipment Research & Development Command ATTN: Dr. J. Bond Mr. D. Dinger Tech Docu Cen, Bldg 315 DRSMR-RZT Fort Belvoir, VA 22060
2	Commander US Army Materiel Development and Readiness Command ATTN: DRCDE-W (J. Corrigan) 5001 Eisenhower Avenue Alexandria, VA 22333	1	Commander US Army Armament Command ATTN: DRSAR-RDT, Dr. T. Hung Rock Island, IL 61201
1	Commander US Army Aviation Systems Command ATTN: DRSAV-E 12th and Spruce Streets St. Louis, MO 63166	2	Commander US Army Picatinny Arsenal ATTN: SARPA-AD-EP Mr. V. Guadagno SARPA-AD-D-A-2 Mr. R. Davitt Dover, NJ 07801
1	Director US Army Air Mobility Research and Development Laboratory Ames Research Center Moffett Field, CA 94035	2	Commander US Army Frankford Arsenal ATTN: SARFA-FCA-W, Mr. D. Swartz SARFA-MDA-A Mr. D. Donnelly Philadelphia, PA 19137

DISTRIBUTION LIST

<u>No. of Copies</u>	<u>Organization</u>	<u>No. of Copies</u>	<u>Organization</u>
1	Commander US Army Rock Island Arsenal ATTN: SARRI-LA-AC, W. Wells Rock Island, IL 61201	1	Deputy Assistant Secretary of the Army (R&D) Department of the Army Washington, DC 20310
1	Commander US Army Watervliet Arsenal ATTN: SARWV-RDD-SE, P. Vottis Watervliet, NJ 12189	1	HQDA (DAMA-ARP) Washington, DC 20310
1	Commander US Army Harry Diamond Labs ATTN: DRXDO-TI 2800 Powder Mill Road Adelphi, MD 20783	1	HQDA (DAMA-MS) Washington, DC 20310
5	Commander US Army Materials and Mechanics Research Center ATTN: DRXMR-T, Mr. J. Bluhm DRXMR-T, Dr. D. Roylance DRXMR-T, Dr. A. F. Wilde Dr. J. Mescall DRXMR-ATL Watertown, MA 02172	1	Chief of Naval Research ATTN: Code ONR 439 N. Perrone Washington, DC 20360
1	Commander US Army Natick Research and Development Command ATTN: DRXRE, Dr. E. Sieling Natick, MA 01761	3	Commander US Naval Air Systems Command ATTN: AIR-604 Washington, DC 20360
1	Director US Army TRADOC Systems Analysis Activity ATTN: ATAA-SA White Sands Missile Range NM 88002	3	Commander US Naval Ordnance Systems Command ATTN: ORD-9132 Washington, DC 20360
1	Commander US Army Research Office ATTN: Dr. E. Saibel P.O. Box 12211 Research Triangle Park NC 27709	2	Commander US Naval Air Development Center, Johnsville Warminster, PA 18974
		1	Commander US Naval Missile Center Point Mugu, CA 93041
		1	Commander and Director David W. Taylor Naval Ship Research & Development Center Bethesda, MD 20084
		2	Commander US Naval Surface Weapons Center Silver Spring, MD 20910

DISTRIBUTION LIST

<u>No. of Copies</u>	<u>Organization</u>	<u>No. of Copies</u>	<u>Organization</u>
4	Commander US Naval Surface Weapons Center ATTN: Code TEB, D. W. Colbertson Mr. L. Hock Code TX, Dr. W. G. Soper Dahlgren, VA 22448	1	AFATL (DLNL, MAJ J. E. Morgan) Eglin AFB, FL 32542
3	Commander US Naval Weapons Center ATTN: Code 4057 Code 5114 Dr. E. Lundstrom Code 6031, Mr. M. Backman China Lake, CA 93555	2	AFWL (WLL) Kirtland AFB, NM 87117
1	Officer in Charge US Naval Weapons Center 3202 E. Foothill Boulevard Pasadena, CA 91107	4	AFFDL (FDT) Wright-Patterson AFB, OH 45433
3	Officer in Charge US Naval Weapons Center Corona Laboratories ATTN: Code 52, Dr. Brown S. G. Plentzas (2 cys) Corona, CA 91720	2	AFML Wright-Patterson AFB, OH 45433
4	Director US Naval Research Laboratory ATTN: Mr. W. J. Ferguson Mr. J. Baker Dr. H. Pusey Dr. F. Rosenthal Washington, DC 20375	1	ASD (YH/EX; John Rievley; XRHD, Gerald Bennett; ENYS, Matt Kolleck) Wright-Patterson AFB, OH 45433
1	Superintendent Naval Postgraduate School ATTN: Dir of Lib Monterey, CA 93940	1	Headquarters National Aeronautics and Space Administration Washington, DC 20546
1	AFOSR (W. J. Walker) Bolling AFB, DC 20332	1	Director Jet Propulsion Laboratory ATTN: Lib (TDS) 4800 Oak Grove Drive Pasadena, CA 91103
1	ADTC/DLJW ATTN: CPT D. Matuska Eglin AFB, FL 32542	2	Director National Aeronautics and Space Administration John F. Kennedy Space Center ATTN: KN-ES-3 KN-ES-34 Kennedy Space Center, FL 32899
4		4	Director National Aeronautics and Space Administration Langley Research Center Langley Station Hampton, VA 23365

DISTRIBUTION LIST

<u>No. of Copies</u>	<u>Organization</u>	<u>No. of Copies</u>	<u>Organization</u>
1	Director National Aeronautics and Space Administration Manned Spacecraft Center ATTN: Lib Houston, TX 77058	3	Honeywell, Inc. Government & Aerospace Products Division ATTN: Mr. J. Blackburn Dr. G. Johnson Mr. R. Simpson 600 Second Street, NE Hopkins, MN 55343
2	Aerospace Corporation ATTN: Mr. R. Kennel Mr. L. G. King P.O. Box 95085 Los Angeles, CA 90045	1	Lockheed Corporation Dept. 8114 ATTN: Dr. C. E. Vivian Sunnyvale, CA 94087
1	Boeing Aerospace Company ATTN: Mr. R. G. Blaisdell (M.S. 40-25) Seattle, WA 98124	2	Mathematical Applications Group, Inc. ATTN: S. Z. Curstein H. S. Schechter 3 Westchester Plaza Elmsford, NY 10523
1	Computer Code Consultants ATTN: Mr. W. Johnson 527 Glencrest Drive Solana Beach, CA 72025	1	McDonnell-Douglas Astronautics Co. ATTN: Mail Station 21-2 Dr. J. Wall 5301 Bolsa Avenue Huntington Beach, CA 92647
2	Dupont Experimental Labs ATTN: Mr. J. Lupton Dr. C. Zweben Wilmington, DE 19801	1	Rockwell Corporation ATTN: Mr. W. Jackson 10301 Overhill Drive Santa Anna, CA 92705
1	Falcon R&D ATTN: Mr. R. Miller 1225 S. Huron Street Denver, CO 80223	3	Sandia Laboratories ATTN: Dr. W. Herrmann Dr. L. Bertholf Dr. J. W. Nunziato P.O. Box 5800 Albuquerque, NM 87115
2	Falcon R&D Thor Facility ATTN: Mr. D. Malick Mr. J. Wilson 696 Fairmount Avenue Baltimore, MD 21204	2	Systems, Science & Software, Inc. ATTN: Dr. R. Sedgwick Ms. L. Hageman P.O. Box 1620 La Jolla, CA 92038
1	President General Research Corporation ATTN: Lib McLean, VA 22101		

DISTRIBUTION LIST

<u>No. of Copies</u>	<u>Organization</u>	<u>No. of Copies</u>	<u>Organization</u>
3	Brown University Division of Engineering ATTN: Prof. P. Marcal Prof. H. Kolsky Prof. P. Symonds Providence, RI 02192	2	Iowa State University Engineering Research Lab ATTN: Dr. G. Nariboli Dr. A. Sedov Ames, IA 50010
2	California Institute of Tech Division of Engineering and Applied Science ATTN: Dr. J. Miklowitz Dr. E. Sternberg Pasadena, CA 91102	2	The Johns Hopkins University ATTN: Dr. J. Bell Dr. R. Green 34th and Charles Streets Baltimore, MD 21218
2	Carnegie Mellon University Department of Mathematics ATTN: Dr. D. Owen Dr. M. E. Gurtin Pittsburg, PA 15213	3	Lehigh University Center for the Application of Mathematics ATTN: Dr. E. Varley Dr. R. Rivlin Dr. A. Kalnins Bethlehem, PA 18015
1	Catholic University of America Schooling of Engineering and Architecture ATTN: Prof. A. Durelli Washington, DC 20017	2	Massachusetts Institute of Technology ATTN: Dr. R. Probstein Dr. J. Dugundji 77 Massachusetts Avenue Cambridge, MA 02139
4	Cornell University Department of Theoretical Applied Mechanics ATTN: Dean E. Cranch Prof. G. Ludford Prof. D. Robinson Prof. Y-H Pai Ithaca, NY 14850	1	New York University Courant Institute ATTN: Dr. S. Z. Burstein 251 Mercer Street New York, NY 10012
2	Drexel University Department of Mechanical Engineering ATTN: Dr. P. C. Chou Dr. F. K. Tsou 32d and Chestnut Streets Philadelphia, PA 19104	1	North Carolina State University Department of Engineering Mechanics ATTN: Dr. W. Bingham P.O. Box 5071 Raleigh, NC 27607
		2	Pennsylvania State University Engineering Mechanical Department ATTN: Prof. Hyathornthwaite Prof. N. Davids University Park, PA 16802

DISTRIBUTION LIST

<u>No. of Copies</u>	<u>Organization</u>	<u>No. of Copies</u>	<u>Organization</u>
2	Forrestal Research Center Aeronautical Engineering Laboratory Princeton University ATTN: Dr. S. Lam Dr. A. Eringen Princeton, NJ 08540	1	Swarthmore College Dept. of Mathematics ATTN: Prof. D. Rosen Swarthmore, PA 19081
1	Purdue University Institute for Mathematical Sciences ATTN: Dr. E. Cumberbatch Lafayette, IN 47907	1	Tulane University Department of Mechanical Engineering ATTN: Dr. S. Cowin New Orleans, LA 70112
2	Purdue University School of Aeronautics, Astronautics and Engineering Sciences ATTN: Prof. S. Koh Prof. C. Sun Lafayette, IN 47907	3	University of Arizona Civil Engineering Department ATTN: Dr. D. A. DaDepo Dr. R. Richard Dr. R. C. Neff Tucson, AZ 85721
2	Rice University ATTN: Dr. Bowen Dr. A. Miele P.O. Box 1892 Houston, TX 77001	2	University of California ATTN: Dr. M. Carroll Dr. P. Naghdi Berkeley, CA 94704
3	Southwest Research Institute Department of Mechanical Sciences ATTN: Dr. U. Lindholm Dr. W. Baker Dr. P. H. Francis 8500 Culebra Road San Antonio, TX 78228	1	University of California Department of Aerospace and Mechanical Engineering Sciences ATTN: Dr. Y. C. Fung P.O. Box 109 La Jolla, CA 92037
1	Stanford Research Institute Poulter Laboratory 333 Ravenswood Avenue Menlo Park, CA 94025	2	University of California Department of Mechanics ATTN: Dr. R. Stern Dr. S. B. Dong 504 Hilgard Avenue Los Angeles, CA 90024
1	Stanford University ATTN: Dr. E. H. Lee Stanford, CA 94305	1	University of Dayton University of Dayton Research Institute ATTN: Mr. H. F. Swift Dayton, OH 45406

DISTRIBUTION LIST

<u>No. of Copies</u>	<u>Organization</u>	<u>No. of Copies</u>	<u>Organization</u>
3	University of Delaware Department of Mechanical Engineering ATTN: Prof. J. Vinson Prof. J. Nowinski Dr. B. Pipes Newark, DE 19711	1	University of Iowa ATTN: Dr. K. Valanis Iowa City, IA 50010
2	University of Denver Denver Research Institute ATTN: Mr. R. F. Recht Mr. T. W. Ipson 2390 South University Boulevard Denver, CO 80210	2	University of Kentucky Department of Engineering Mechanics ATTN: Dr. M. Beatty Prof. P. Gillis Lexington, KY 40506
3	University of Florida Department of Engineering Science and Mechanics ATTN: Dr. C. A. Sciammarella Dr. L. Malvern Dr. N. Cristescu Gainesville, FL 32601	2	University of Maryland Department of Mechanical Engineering ATTN: Prof. Y. Yang Dr. J. Dally College Park, MD 20742
1	University of Houston Department of Mechanical Engineering ATTN: Dr. R. Nachlinger Houston, TX 77004	1	University of Minnesota Department of Engineering Mechanics ATTN: Dr. R. Fosdick Minneapolis, MN 55455
1	University of Illinois at Chicago Circle College of Engineering Department of Materials Engineering ATTN: Prof. A. Schultz P.O. Box 4348 Chicago, IL 60680	4	University of Texas Department of Engineering Mechanics ATTN: Dr. C. H. Yew Prof. Ripperger Prof. Bedford Dr. J. T. Oden Austin, TX 78712
1	University of Illinois Department of Theoretical and Applied Mechanics ATTN: Dr. D. Carlson Urbana, IL 61801	1	University of Washington Department of Mechanical Engineering ATTN: Prof. J. Chalupnik Seattle, WA 98105
		1	Washington State University Department of Physics ATTN: Dr. G. E. Duvall Pullman, WA 99163

DISTRIBUTION LIST

No. of <u>Copies</u>	<u>Organization</u>
2	Yale University ATTN: Dr. B. Chu Dr. E. Onat 400 Temple Street New Haven, CT 96520

Aberdeen Proving Ground

Marine Corps Ln Ofc
Cdr, USATECOM
ATTN: Mr. W. Pless
Mr. S. Keithley
Dir, USAMSA
ATTN: Dr. Sperrazza
Mr. Nolan
Mr. Brooks